Caloric curve and conditional moments: Effects of secondary fragment decay

P. F. Mastinu
Dipartimento di Fisica and INFN, Via Irnerio 46, I-40126 Bologna, Italy

M. Belkacem
Institut für Theoretische Physik, J. W. Goethe-Universität, D-60054 Frankfurt am Main, Germany

F. Gramegna
INFN, Laboratori Nazionali di Legnaro, I-35020 Legnaro (Pd), Italy

P. M. Milazzo
Dipartimento di Fisica and INFN, Via Valerio 2, I-34127 Trieste, Italy

(Received 14 May 1997)

We establish, within the framework of the statistical multifragmentation model, the connection between the caloric curve and the analysis of conditional moments. In particular, we show that the conditional moments of fragment charge distributions peak at the region where the curve temperature versus excitation energy shows a plateau assumed to be a signature of a phase transition. Furthermore, we show that the slopes of the moments at the peak are not influenced by secondary decay after the first breakup of the nucleus. [S0556-2813(98)04901-2]

PACS number(s): 25.70.Pq, 24.10.Pa, 25.70.Mn, 25.75.−q

I. INTRODUCTION

Nuclear multifragmentation and its possible connection to the occurrence of a liquid-gas phase transition has been the subject of intensive investigations, both theoretical and experimental, for more than a decade [1–7]. Theoretical studies indicate that infinite nuclear matter has an equation of state very similar to that of a van der Waals gas [8–11]. Moreover, recent experimental results show strong evidence for the occurrence of a phase transition in fragmenting nuclear systems. These results can be arbitrarily classified in two main groups: (i) In first place those related to the characterization of the phase transition using the analysis of moments of asymptotic cluster size distributions [12,13]; (ii) The second regards the measurement of the caloric curve of nuclear fragmenting systems, reminiscent of the behavior of a liquid-gas system [14].

In the present paper, using the statistical multifragmentation model (SMM) [15–17], we study the connection between the particular shape of the caloric curve which shows the variation of the temperature in function of the excitation energy, and the analysis of conditional moments introduced by Campi [18] to characterize the critical behavior of a system. We show in particular that the appearance of peaks (or maxima) in the plots of the moments occurs in the same excitation energy or temperature interval where one observes a plateau in the caloric curve supposed to be a signature of a phase transition. We then analyze the effects of secondary decay on the particular shape of the peaks appearing in the conditional moments after the first breakup of the system. We show that secondary decay does not affect the behavior of the moments around the peaks.

In our study, we pay special attention to the analysis of the different signals versus charged particle multiplicity (experimentally used as the measure from the critical point [12]). Other authors have studied the effects of preequilibrium on charged particle multiplicity distributions [19–22]. In this paper indeed, we would like to discuss the effects on these distributions induced by secondary decay. We show in particular that within this model, charged particle multiplicity is not linearly related to the temperature. Moreover, by looking at the signals as a function of charged particle multiplicity, it is found that while secondary decay does not change the qualitative shape of the different signals, it induces some changes in the slopes of the different moments near the peak.

In Sec. II, we briefly review the SMM model used in this paper. Section III deals with the study of the correlation between the caloric curve and the conditional moments analysis at freeze-out time, before secondary decay takes place. We study in Sec. IV the effects of secondary decay on the different signals. The analysis versus charged particle multiplicity is also done in this section. Finally, conclusions are drawn in Sec. V.

II. THE SMM MODEL

The statistical multifragmentation model is based on the assumption of statistical equilibrium at a low density freeze-out stage of the nuclear system formed during the collision. At this stage, primary fragments are formed according to their equilibrium partitions. Equilibrium partitions are calculated according to the microcanonical ensemble of all breakup channels composed of nucleons and excited fragments of different masses. The model conserves total excitation energy, momentum, mass, and charge numbers. The statistical weight of decay channel j is given by $W_j \propto \exp[S_j(E_s^*, V_s, A_s, Z_s)]$, where S_j is the entropy of the system in channel j and E_s^*, V_s, A_s, and Z_s are the excitation energy, volume, mass, and charge numbers of the fragment-

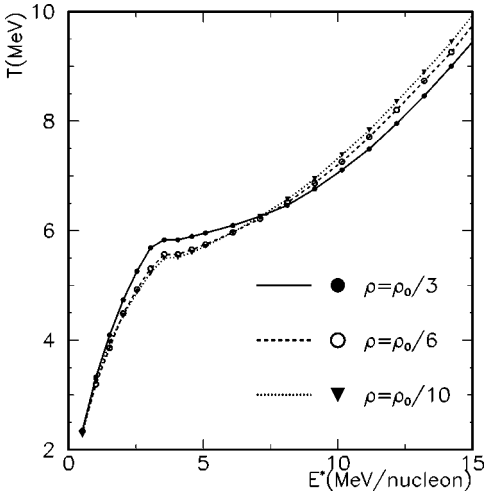

FIG. 1. Caloric curve: temperature versus excitation energy for a Au nucleus, for different values of nuclear density at freeze-out.

ing source. Different breakup configurations are initialized according to their statistical weights. The fragments are then propagated in their mutual Coulomb field and allowed to undergo secondary decay. Light fragments with mass number $A_f \leqslant 4$ are considered as stable particles with only translational degrees of freedom; fragments with $A_f > 4$ are treated as heated nuclear liquid drops. The secondary decay of large fragments ($A_f > 16$) is calculated from an evaporation-fission model, and that of smaller fragments from a Fermi breakup model [16]. The present version of the model only incorporates thermal degrees of freedom and does not take into account any additional collective degrees of freedom such as radial expansion or angular momentum (for more details, see Refs. [15–17]).

In the following we study the fragmentation of a gold $^{197}_{79}$Au nucleus at different excitation energies. In Fig. 1, we have plotted the temperature T obtained from the model versus excitation energy E^* for different freeze-out densities ρ_f. This plot is commonly called the caloric curve [14–16]. All curves show the same shape which starts by increasing with excitation energy, then one observes a ''back-bending'' at almost the same excitation energy $E^* = 3 - 3.5$ MeV for all curves after which the temperature increases very slowly as a function of excitation energy till an excitation energy of about 8 MeV. Then temperature increases rapidly with excitation energy. This flattening of the caloric curve, observed also experimentally in the fragmentation of the quasiprojectile formed in the collision Au on Au at 600 MeV/nucleon, is thought to be reminiscent of the behavior of a liquid-gas system [14,16]. In the following, the discussion will deal on the model predictions at a fixed freeze-out density of the emitting source of $\rho_f = \rho_0/3$; no different behavior was found at smaller freeze-out densities.

III. STUDY OF SIGNALS AT FREEZE-OUT TIME

Figure 2 shows the contour plot of charged particle multiplicity N_c versus excitation energy E^* (upper panel of the figure) and versus temperature T (lower panel) taking into account secondary decay. We note that even if experimentally it is possible to measure N_c only in the final stage of the

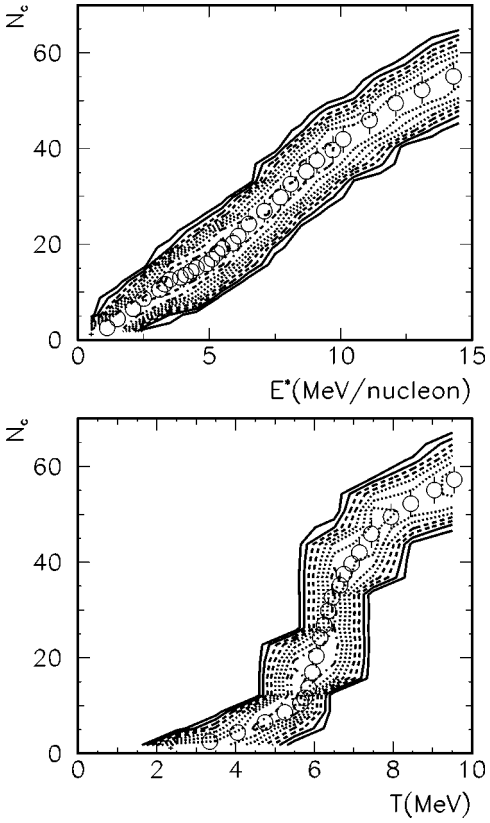

FIG. 2. Total number of charged particles at the end of the de-excitation chain as a function of temperature (lower panel) and excitation energy (upper panel) of the emitting source. The curves with solid circles represent the average values of charged particle multiplicity.

reaction, we checked that the shape of the previous plot is not modified by secondary decay. From the plot, one observes that while in average N_c increases almost linearly with excitation energy, it shows large fluctuations around the mean value. If one makes a narrow cut on N_c, say $39 \leqslant N_c \leqslant 40$, this will correspond mainly to events with $E^* = 9 - 10$ MeV, but events with E^* from 7 to 12 MeV fall also within the cut. The situation is the same versus temperature where however, one observes very large fluctuations of N_c at temperature $T \approx 6$ MeV (temperature of the plateau in the caloric curve).

Moreover, while N_c shows in average a linear dependence versus E^* (solid points), it does not show this dependence versus temperature T. N_c should then be considered proportional to E^* rather than T. This indicates that one has to be careful when extracting critical exponents for a thermal phase transition using charged particle multiplicity as an indicator of the distance to the critical point. Furthermore, charged particle multiplicity N_c cannot be properly used as an indicator of the characteristics of the analyzed source (which selects a given temperature T or excitation energy E^* or impact parameter b). In fact, N_c is proportional to E^* or T or b (if any) only in the average and most of the signals proposed to give evidence for the critical behavior are mainly based on the assumption that the fluctuations are the largest at the critical point (this in fact could be observed in the plot of N_c versus T of Fig. 2 at $T \sim 6$ MeV). Making narrow cuts on N_c to select small windows in temperature or

excitation energy means cutting down the fluctuations which are the principal argument when studying phase transitions.

In the following part of this section the calculations are carried out without secondary decay. In all the figures also, while the curves with solid dots indicate the signals at freeze-out, the curves with open circle markers (when plotted) indicate the same signals after secondary decay.

The method of conditional moments has been introduced by Campi to characterize the critical behavior of a system undergoing a multifragmentation [18]. The moments of fragment charge distributions are defined as

$$M_k^{(j)} = \sum_z Z^k n^{(j)}(Z)/Z_{\rm tot}, \tag{1}$$

where $n^{(j)}(Z)$ is the multiplicity of clusters of charge Z in the event j, $Z_{\rm tot}=79$, and the sum is over all fragments in the event *except the heaviest one*, which corresponds to the bulk in an infinite system. Assuming a general scaling property of cluster size distributions near the critical point [23], one gets for the moments near the critical point

$$M_k \propto |T-T_c|^{-(1+k-\tau)/\sigma}. \tag{2}$$

Since the exponent τ satisfies $2<\tau<3$, the second and higher moments diverge at the critical point, while the lower moments M_0 (mean number of fragments) and M_1 (mean size) do not. In particular, the second moment M_2 (variance of charge distributions), which in macroscopic thermal systems is proportional to the isothermal compressibility, diverges at the critical point [23–25]. Of course, in finite systems, the moments M_k remain finite, even for $k>1$.

Our aim in this section is to show the close connection between the appearance of peaks or maxima in the plots of conditional moments of cluster size distributions and the flattening we have observed in the caloric curve (Fig. 1). Figure 3 shows the second moment M_2 versus temperature T (upper part) and versus excitation energy E^* (lower part). One observes in the upper part of the figure a sharp peak with a sudden rise of M_2 (with almost an infinite slope) at $T\approx 6$ MeV, the temperature at which the caloric curve shows a plateau. The same is for M_2 versus excitation energy E^*, but the peak is broader and spreads over the excitation energy range which corresponds to the plateau.

We observe the same behavior in the plot of the relative variance γ_2 shown in Fig. 4. This quantity, defined as [18]

$$\gamma_2 = \frac{M_2 M_0}{M_1^2}, \tag{3}$$

has been also proposed by Campi to better characterize the critical region. In particular, it is expected that this quantity shows a maximum around the critical point meaning that the fluctuations of fragment size distributions are the largest near the critical point. The relative variance (Fig. 4), as with the second moment, shows the same sharp peak around $T\approx 6$ MeV, which becomes broader versus excitation energy. Here also we note that the peak shows up in the same excitation energy interval of the plateau in the caloric curve.

We consider another variable which we think is a good signal worthwhile to analyze to characterize the irregular behavior at the critical point. This quantity is the ratio of the first conditional moment M_1 to the zeroth moment M_0. According to Eq. (2), both moments M_0 and M_1 do not diverge at the critical point and have a regular behavior. However, their ratio is no longer regular and behaves as

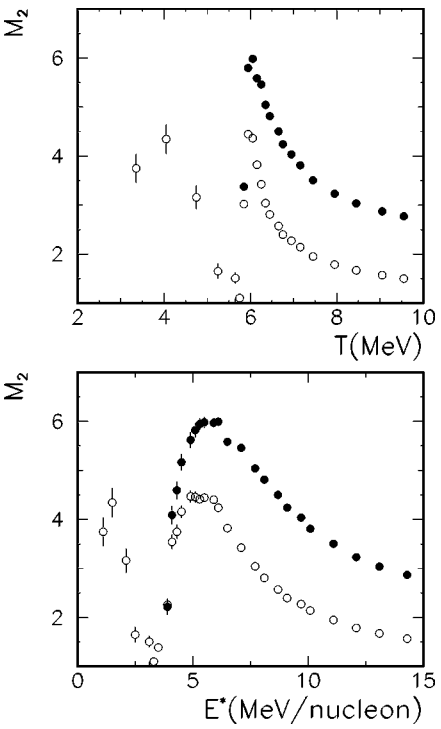

FIG. 3. Second moment of charge distributions as a function of temperature and excitation energy without (solid points) and with (open circles) secondary decay.

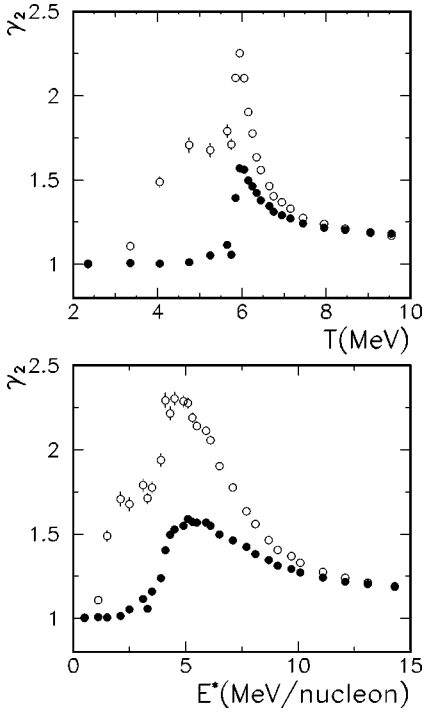

FIG. 4. Relative variance of charge distributions versus temperature and excitation energy without (solid points) and with (open circles) secondary decay.

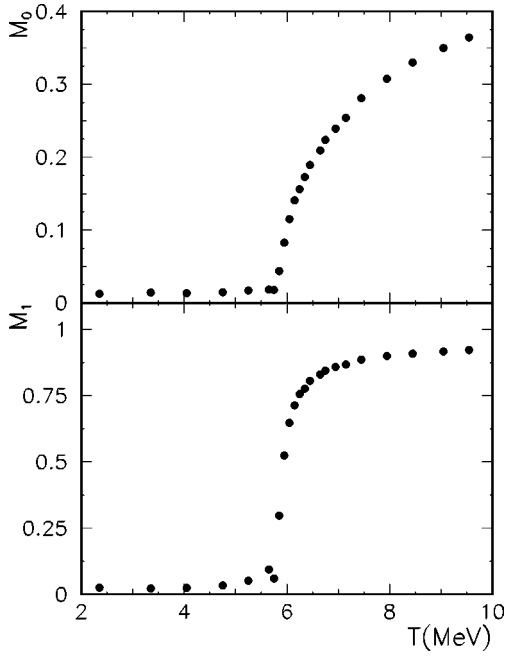

FIG. 5. First- and zeroth-order moments of charge distributions as a function of temperature before secondary decay.

$$\frac{M_1}{M_0} = |T - T_c|^{-1/\sigma}. \tag{4}$$

As $\sigma > 0$ [18,23], the ratio diverges at the critical point. In Fig. 5, we have plotted M_0 (upper part) and M_1 (lower part) versus temperature T. Both quantities show no maximum and have a regular behavior. Their ratio, however, plotted in the upper part of Fig. 6 versus T, shows a peak at temperature $T \approx 6$ MeV.

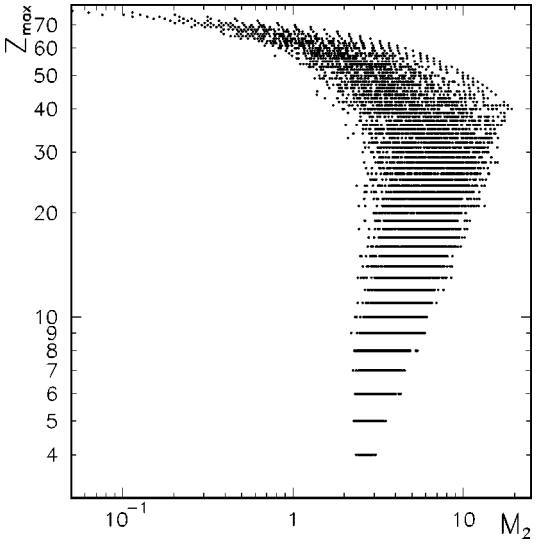

FIG. 7. Campi scatter plot: The charge of the largest fragment is plotted versus the second moment.

The Campi scatter plot drawn in Fig. 7 exhibits the peculiar shape expected for the occurrence of a phase transition. Each point of the plot represents one event. This figure shows that the whole accessible $Z_{\max}$-M_2 space is filled up. We stress, however, that the central region of this plot (the zone where the upper branch crosses the lower branch, supposed to correspond to critical events [18,26]) is mainly made by events having temperature T between 5.8 and 6.2 MeV. The normalized variance of the size of the maximum fragment σ_{NV} is also drawn in Fig. 8. Because fragment charge distributions are expected to show the maximum fluc-

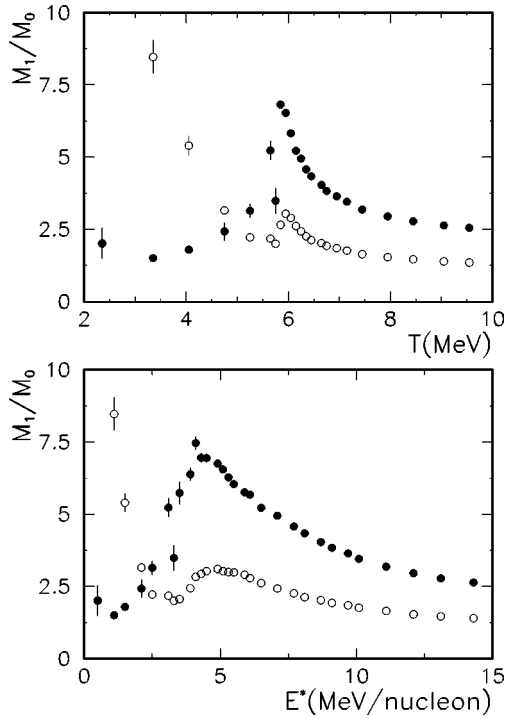

FIG. 6. Ratio of first moment to zeroth moment of charge distributions versus temperature and excitation energy without (solid points) and with (open circles) secondary decay.

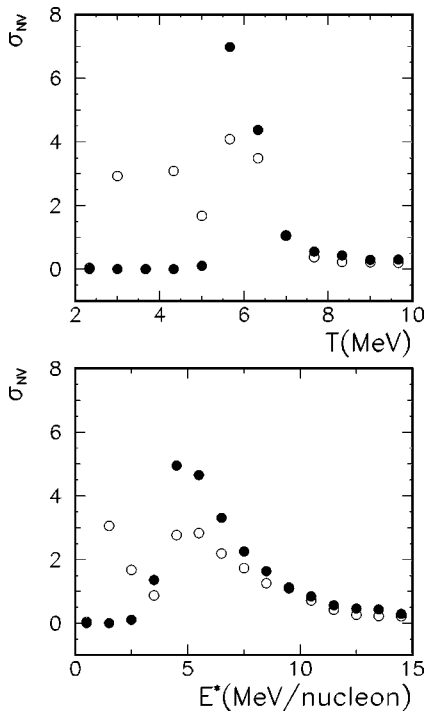

FIG. 8. Normalized variance of the charge of the largest fragment versus temperature and excitation energy without (solid points) and with (open circles) secondary decay.

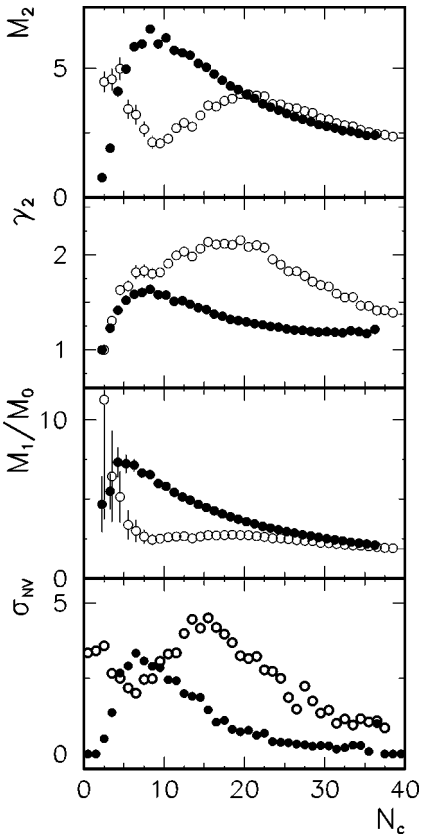

FIG. 9. Various signals as a function of the total number of charged emitted particles without (solid points) and with (open circles) secondary decay.

tuations around the critical point, this variable should show a maximum in the critical region [18,23]. The normalized variance, which is related to the fluctuation of the order parameter, is defined as

$$\sigma_{NV}=\frac{\sigma^2_{Z_{\max}}}{\langle Z_{\max}\rangle}, \quad \sigma^2_{Z_{\max}}=\langle Z^2_{\max}\rangle-\langle Z_{\max}\rangle^2. \tag{5}$$

As expected, σ_{NV} shows a huge maximum versus temperature or excitation energy, at the same values where the conditional moments peaked.

Before ending this section, we would like to note that all previous signals when plotted versus charged particle multiplicity, show broad peaks which spread over the whole multiplicity range corresponding to the plateau in the caloric curve ($4\leqslant N_c\leqslant 13$, see Fig. 9).

IV. EFFECTS OF SECONDARY DECAY

In the preceding section, we have seen that the analysis of conditional moments after the first breakup of the system indicates the occurrence of a critical behavior in the temperature-excitation energy interval where the caloric curve shows a plateau. As from the experimental point of view, the only accessible quantities are the asymptotic fragment charge distributions, we will revisit in this section the previous signals and study the effects of secondary decay.

From Figs. 3, 4, 6, and 8, we see that secondary decay changes the slope of the various quantities only far from the peak (curves with open circles), while near the peak, the slope of the increasing branch does not change significantly. Note that in all the plots, due to secondary decay, a smaller peak appears at small values of temperature and excitation energy. This bump is due to the presence of fission fragments, produced in secondary decay. In all cases, the behavior of the signals near the singularity seems not to change significantly both versus T or E^*.

The situation is different when the different signals are plotted versus charged particle multiplicity. Figure 9 shows the different signals plotted versus N_c at freeze-out (solid points) and after secondary decay (open circles). First, one sees that the position of the peak is no longer the same before and after secondary decay. This is obvious because N_c increases after the primary excited fragments de-excite by emitting smaller fragments. One notes also the presence (in the curves with secondary decay) of the second bump at low N_c's characteristic of fission events. One observes also an important change on the slope of the increasing branch. While the qualitative behavior of the plot (the presence of a peak) remains, the extraction of critical exponents from the plot of the second moment, for example, by fitting the slopes of the peak cannot be considered completely correct, because their values would be different if calculated before and after secondary decay.

These results indicate that (i) secondary decay which represents a regular behavior of the system does not change the behavior of the different signals at the peak when plotted versus temperature or excitation energy. This would happen only if the peak is associated with a nonanalytic behavior (expected at the singularity point of a second order phase transition) which would not be affected by a regular one; (ii) the slopes of the increasing branches in the different signal change significantly before and after secondary decay when plotted versus multiplicity. This is due to the fact that secondary decay changes not only the absolute values of the signals (y axis) but also changes the absolute value of charged particle multiplicity, and hence even if point (i) applies, the slopes of the peaks before and after secondary decay will be different due to the change in the multiplicity of charged particles.

V. DISCUSSION AND CONCLUSIONS

In this paper, we have shown that all studied signals indicate a clear connection between the conditional moments analysis and the caloric curve. All moments peak in the same temperature-excitation energy region where the flattening of the caloric curve is observed, indicating a strong correlation between the two methods proposed so far to characterize the occurrence of a possible phase transition in nuclear collisions. Moreover, while the analysis of conditional moments has been introduced to characterize the behavior of nuclear systems in the vicinity of a critical point indicating the occurrence of a second-order phase transition [12,18], the observation of the flattening in the caloric curve was supposed to be reminiscent of a first-order phase transition [14,16]. From our analysis, we believe that the actual shape of the caloric curve corresponds indeed to a second-order phase transition characterized by a critical temperature, the temperature at which the flattening is observed. In fact, it ap-

pears that the observed sharp peaks of the moments are observed at the temperature of the plateau in the caloric curve. These peaks when observed versus excitation energy, spread over the entire excitation energy interval of the plateau (although the ratio M_1/M_0 shows a less broader bump peaking at an excitation energy of about 4–4.5 MeV). This observation is supported by the fact that secondary decay does not affect significantly the slopes of the increasing branch in the different signals, which would happen only if the peak is associated with a singularity expected at the critical point of a phase transition.

It appears also that the analysis of conditional moments versus charged particle multiplicity N_c is only qualitatively correct, in the sense that the presence of peaks in the various variables (which indicates that the system has passed through the critical point) remains even after the secondary decay, but a quantitative analysis can only be done versus temperature or excitation energy. In particular, the extraction of critical exponents versus charged particle multiplicity from asymptotic charge distributions would not be completely correct because charged particle multiplicity appears not to be linearly dependent on temperature (in average) and the slopes of the different conditional moments change significantly before and after secondary decay.

ACKNOWLEDGMENTS

The authors thank Dr. A. S. Botvina for providing us with his version of the SMM code, and for fruitful and stimulating discussions. One of us (M.B.) thanks the Alexander von Humboldt-Stiftung for financial support and the Institut für Theoretische Physik of Frankfurt University for kind hospitality.

[1] M. W. Curtain, H. Toki, and D. K. Scott, Phys. Lett. **123B**, 289 (1983); A. D. Panagiotou, M. W. Curtain, H. Toki, D. K. Scott, and P. J. Siemens, Phys. Rev. Lett. **52**, 496 (1984).
[2] G. F. Bertsch and P. J. Siemens, Phys. Lett. **126B**, 9 (1983).
[3] A. L. Goodman, J. I. Kapusta, and A. Z. Mekjian, Phys. Rev. C **30**, 851 (1984).
[4] H. R. Jaqaman, Gabor Papp, and D. H. E. Gross, Nucl. Phys. **A514**, 327 (1990).
[5] B. Jakobsson, G. Jönsson, B. Lindkvist, and A. Oskarsson, Z. Phys. A **307**, 293 (1982); B. Jakobsson *et al.*, Nucl. Phys. **A509**, 195 (1990).
[6] H. H. Gutbrod, A. I. Warwick, and H. Wieman, Nucl. Phys. **A387**, 177c (1982); A. D. Panagiotou, M. W. Curtin, and D. K. Scott, Phys. Rev. C **31**, 55 (1985); W. G. Lynch, Annu. Rev. Nucl. Part. Sci. **37**, 493 (1987); L. G. Moretto, *ibid.* **43**, 379 (1993).
[7] J. E. Finn *et al.*, Phys. Rev. Lett. **49**, 1321 (1982); Phys. Lett. **118B**, 458 (1982); H. H. Gutbrod, A. I. Warwick, and H. Wieman, Nucl. Phys. **A387**, 177c (1982); A. S. Hirsch *et al.*, Phys. Rev. C **29**, 508 (1984); M. Mahi, A. T. Bujak, D. D. Carmony, Y. H. Chung, L. J. Gutay, A. S. Hirsch, G. L. Paderewski, N. T. Porile, T. C. Sangster, R. P. Scharenberg, and B. C. Stringfellow, Phys. Rev. Lett. **60**, 1936 (1988).
[8] R. G. Palmer and P. W. Anderson, Phys. Rev. D **9**, 3281 (1974); W. G. Kupper, G. Wegmann, and E. R. Hilf, Ann. Phys. (N.Y.) **88**, 454 (1974); S. A. Chin and J. D. Walecka, Phys. Lett. **52B**, 24 (1974).
[9] U. Mosel, P. G. Zint, and K. H. Passler, Nucl. Phys. **A236**, 252 (1974); G. Sauer, H. Chandra, and U. Mosel, *ibid.* **A264**, 221 (1976).
[10] D. Q. Lamb, J. M. Lattimer, C. J. Pethick, and D. G. Ravenhall, Phys. Lett. **41**, 1623 (1978); Nucl. Phys. **A360**, 459 (1981); P. Danielewicz, *ibid.* **A314**, 465 (1979); H. Schulz, L. Münchow, G. Röpke, and M. Schmidt, Phys. Lett. **119B**, 12 (1982); Nucl. Phys. **A399**, 587 (1983).
[11] H. R. Jaqaman, A. Z. Mekjian, and L. Zamick, Phys. Rev. C **27**, 2782 (1983); **29**, 2067 (1984).
[12] J. B. Elliot, M. L. Gilkes, J. A. Hauger, A. S. Hirsch, E. Hjort, N. T. Porile, R. P. Scharenberg, B. K. Srivastava, M. L. Tincknell, and P. G. Warren, Phys. Rev. C **49**, 3185 (1994); M. L. Gilkes *et al.*, Phys. Rev. Lett. **73**, 1590 (1994).
[13] P. F. Mastinu *et al.*, Phys. Rev. Lett. **76**, 2646 (1996); P. F. Mastinu *et al.*, *XXXIV International Winter Meeting on Nuclear Physics*, Bormio, 1996, edited by I. Iori (unpublished), p. 110.
[14] J. Pochodzalla *et al.*, Phys. Rev. Lett. **75**, 1040 (1995).
[15] J. Bondorf, R. Donangelo, I. N. Mishutsin, and H. Schulz, Nucl. Phys. **A444**, 460 (1985).
[16] J. P. Bondorf, A. S. Botvina, A. S. Iljinov, I. N. Mishustin, and K. Sneppen, Phys. Rep. **257**, 133 (1995).
[17] A. S. Botvina *et al.*, Nucl. Phys. **A475**, 663 (1987).
[18] X. Campi, J. Phys. A **19**, L917 (1986); Phys. Lett. B **208**, 351 (1988); J. Phys. (France) **50**, 183 (1989).
[19] Y. Yariv and Z. Fraenkel, Phys. Rev. C **20**, 2227 (1979).
[20] R. Charity *et al.*, Nucl. Phys. **A483**, 371 (1988).
[21] D. Cussol *et al.*, Nucl. Phys. **A561**, 298 (1993).
[22] W. Bauer and A. Botvina, Phys. Rev. C **52**, R1760 (1995).
[23] D. Stauffer, Phys. Rep. **54**, 1 (1979).
[24] R. Balescu, *Equilibrium and Nonequilibrium Statistical Mechanics* (Krieger, Malabar, FL, 1991).
[25] P. Finocchiaro, M. Belkacem, T. Kubo, V. Latora, and A. Bonasera, Nucl. Phys. **A600**, 236 (1996).
[26] M. Belkacem, V. Latora, and A. Bonasera, Phys. Rev. C **52**, 271 (1995).